DOI: 10.1002/chem.200700847

Assessing the Mechanical Properties of a Molecular Spring

Emanuela Berni,[a] Brice Kauffmann,[a] Chunyan Bao,[a] Julien Lefeuvre,[a] Dario M. Bassani,[b] and Ivan Huc*[a]

Abstract: We report on the dramatic effect of increasing helix diameter on the hybridization of oligopyridine-dicarboxamide strands into double helices. Upon replacing a single pyridine by a 1,8-diazaanthracene unit within an oligomeric strand, a 4.7 Å enlargement of the helix diameter occurs parallel to the long anthracene axis. This structure change results in a spectacular stabilization of the double helical hybrids derived from these strands (factors of over 10^7). Detailed investigations of the hybridization process using X-ray crystallography, NMR, fluorescence measurements and molecular mechanics calculations allowed us to assign the duplex stabilization to two enthalpic effects. First, the increase in diameter results in an augmented surface, involved in intermolecular π–π stacking. Second, the enlarged diameter leads to a lower tilt angle of the helical strand, with respect to the helix axis, which in turn results in smaller dihedral angles at the aryl–amide linkages and thus a considerably lowered enthalpic cost of the spring-like extension of the strands during the hybridization process. These results provide novel insights into how subtle tuning of molecular components may result in considerable and rationalizable changes in double helical supramolecular architectures.

Keywords: helical structures · molecular recognition · structure elucidation · supramolecular chemistry

Introduction

Current interest for artificial molecular machines is shedding new light on the resemblances and differences between human and molecular scale mechanical devices.[1] One essential component, which forms the basis of numerous mechanical systems, is the helical spring. For springs that follow Hooke's Law, the spring constant k, which expresses the resistance to elongation (i.e., to the shear that elongation causes in the material), is dependent on several parameters [Eq. (1)].[2]

$$k = G\frac{d^4}{8nD^3} \quad (1)$$

In Equation (1), G is the material shear modulus, n is the number of coils, D the spring diameter, and d the thickness of the coiled wire (Scheme 1). At the molecular scale, helically coiled folded conformations are widespread and have received considerable attention.[3] However, the potential resemblance between molecular helices and springs is still largely unexplored, except for DNA, which has been the object of numerous single molecule manipulations (e.g., stretching).[4] Here, we report experimental evidence that the resistance of some molecular helices to elongation is, as for springs, strongly lowered upon increasing helix diameter (D in Equation (1)).

These findings came at the conclusion of a study of the dramatic effect of increasing the helix diameter on the hy-

[a] Dr. E. Berni, Dr. B. Kauffmann, Dr. C. Bao, J. Lefeuvre, Dr. I. Huc
Université Bordeaux 1 - ENITAB - CNRS UMR5248
Institut Européen, de Chimie et Biologie
2 rue Robert Escarpit, 33607 Pessac (France)
Fax: (+33) 540-002-215
E-mail: i.huc@iecb.u-bordeaux.fr

[b] Dr. D. M. Bassani
Université Bordeaux 1 - CNRS UMR5255
Institut des Sciences Moléculaires
351 cours de la Libération, 33405 Talence (France)

Supporting information for this article is available on the WWW under http://www.chemeurj.org/ or from the author.

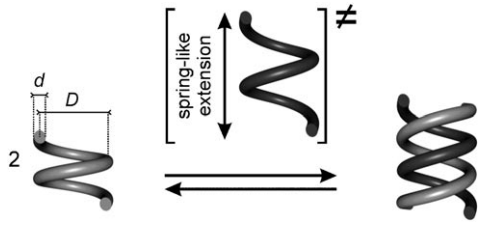

Scheme 1. Representation of the extension of a molecular spring leading to formation of a double helical dimer (D = spring diameter; d = thickness of the coiled wire).

bridization of oligopyridine-dicarboxamide strands into double helices. Despite their familiar nature, double helices, consisting of two intertwined organic oligomeric or polymeric strands, largely remain intractable objects. Observations thereof have, thus, resulted from serendipity[5,6] more often than from rational design,[7] unless they are directly inspired from natural examples as gramicidin[8] or DNA.[9,10] Unlike more robust supramolecular architectures such as, self-assembled molecular capsules,[11] their structure and stability depends, in nontrivial terms, on the geometrical parameters imparted by each monomer in the sequence. For example, the pioneering work by Eschenmoser et al. showed that the helical pitch, base-pairing mode, and stability of double helices of nucleic acid analogues are greatly altered upon replacing ribose by other sugars.[10] The results reported here, and the analogy between molecular helices and springs, thus provide novel insights on how subtle tuning of molecular components results in considerable and rationalizable changes in helical supramolecular architectures and their conformational properties.

Results and Discussion

Molecular design: In solution, oligoamides of 2,6-diaminopyridine and 2,6-pyridinedicarboxylic acid fold into stable single helical conformations, and hybridize into double helices stabilized by interstrand π–π interactions.[6,12] For example, the previously described oligomer **1** (Figure 1) has a di-

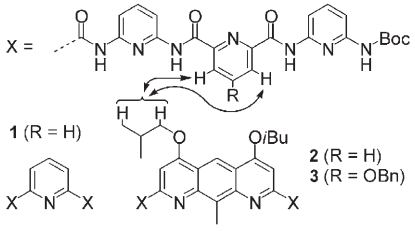

Figure 1. Structures of oligomers **1**–**3**. The double headed arrows show selected correlations observed in 400 MHz ROESY ^{1}H NMR spectra of **2**.

merization constant (K_{dim}) of 100 L mol^{-1} in $CDCl_3$.[6] The hybridization process implies a spring-like extension of the helix length to double the helical pitch from 3.5 to 7 Å as depicted in Scheme 1. Modeling studies suggest that hybridization proceeds through a slippage mechanism involving a series of roller-coaster like discrete steps.[12a] Intramolecular π–π stacking interactions within the single helical monomers are replaced by intermolecular aromatic stacking after the tail of one of the strands proceeds inside the other single helical strand in an eddy-like process.

In the context of research aiming at performing host–guest chemistry in the hollows of helical conformers,[13] we designed structurally related monomers larger than 2,6-pyridinedicarboxylic acid so as to increase helix diameter. Thus, a 1,8-diazaanthracene-2,7-dicarboxylic acid was prepared and incorporated in heptamer **2** (see below). This oligomer was considered a simple synthetic intermediate until we discovered its unprecedented hybridization properties (see below). Its structure differs from that of **1** only in that the central pyridine is replaced by a 1,8-diazaanthracene monomer. Molecular models show that this change should lead to a 4.7 Å enlargement of helix diameter parallel to the long anthracene axis, but should have no effect on the helical pitch and on the curvature at each unit, which determines the number of units per turn.

Synthesis: Oligomers **2** and **3** were prepared using a convergent approach as depicted in Scheme 2. Precursor **4** was ob-

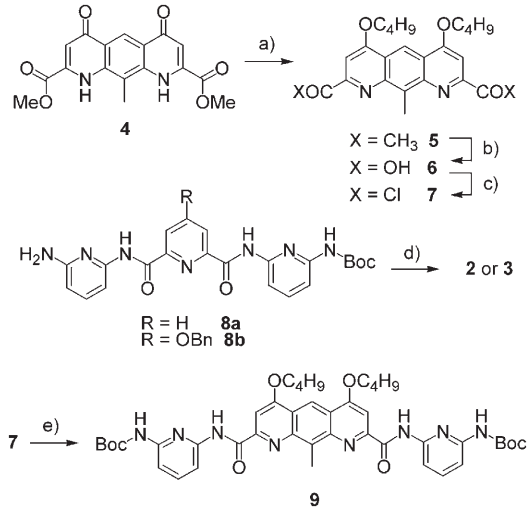

Scheme 2. a) *i*BuOH, PPh_3, diisopropylazadicarboxylate, THF, 90% yield; b) NaOH, dioxane/water, quant.; c) 1-chloro-*N*,*N*-2-trimethylpropenylamine, $CHCl_3$, quant.; d) **7**, DIEA, THF, 66–71%; e) 2-amino-6-*tert*-butoxycarbonylaminopyridine, DIEA, CH_2Cl_2, 53%.

tained in two steps from 2,6-diaminotoluene and dimethyl acetylenedicarboxylate following the described procedures.[14] Precursor **4** was converted to 1,8-diazaanthracene[15] **5** under Mitsunobu conditions. Saponification of the two ester functions of **5** and conversion of the subsequent diacid into a diacid chloride yielded **7**, which was consequently coupled to monoamines **8a**, or **8b** or to 2-amino-6-*ter*butoxycarbonylamino-pyridine to give heptamer **2**, heptamer **3**, or trimer **9**, respectively. The latter, **9**, was used as a nonhelical reference for the chemical shift values.

Solid-state studies: The solid-state structure of **2** was solved from three different crystals obtained from pure MeOH, pure DMSO, and toluene/hexane, respectively (Table 1). All structures showed a double helical architecture, which was not anticipated in this series (Figure 2). Indeed, the hybridization of aromatic carboxamide oligomers had up to now appeared to be notoriously sensitive to structural changes and, besides the original pyridine rings, pyridine *N*-oxides have been the only other rings that we were able to introduce without disrupting the duplexes.[12e,f]

Table 1. Crystallographic parameters for the three structures of **2** determined.

	2	**2**	**2**
solvent of crystalisation	toluene/hexane	DMSO	MeOH
formula	$C_{143}H_{148}N_{32}O_{26}$	$C_{292}H_{308}N_{64}O_{77}S_6$	$C_{145.50}H_{136}N_{32}O_{36.50}$
dimensions [mm]	$0.2\times0.2\times0.4$	$0.5\times0.5\times0.5$	$0.3\times0.2\times0.5$
color	yellow	yellow	yellow
crystal system	monoclinic	monoclinic	triclinic
space group	$P2_1/c$	$C2/c$	$P-1$
Z	4	8	2
a [Å]	17.8590(10)	47.476(2)	19.6090(10)
b [Å]	28.8820(10)	28.2530(10)	19.9000(10)
c [Å]	33.1520(10)	27.0690(10)	22.5920(10)
α [°]	90	90	96.141(4)
β [°]	100.257(2)	110.440(3)	114.233(3)
γ [°]	90	90	104.144(4)
t [K]	153	153	153(2)
V [Å^3]	16826.6(12)	34023(2)	7578.1(6)
ρ [g cm^{-3}]	1.078	1.198	1.278
λ, E	1.54178	1.54178	1.54178
θ measured [°]	$2.94\le\theta\le72.57$	$6.56\le\theta\le72.16$	$6.53\le\theta\le72.11$
reflns measured	113280	128214	106986
unique reflns	27697	28492	26349
GOF	1.492	1.127	0.974
R_1 [$I>2\sigma(I)$]	0.1832	0.1270	0.0798
wR_2 (all data)	0.4332	0.4140	0.2733

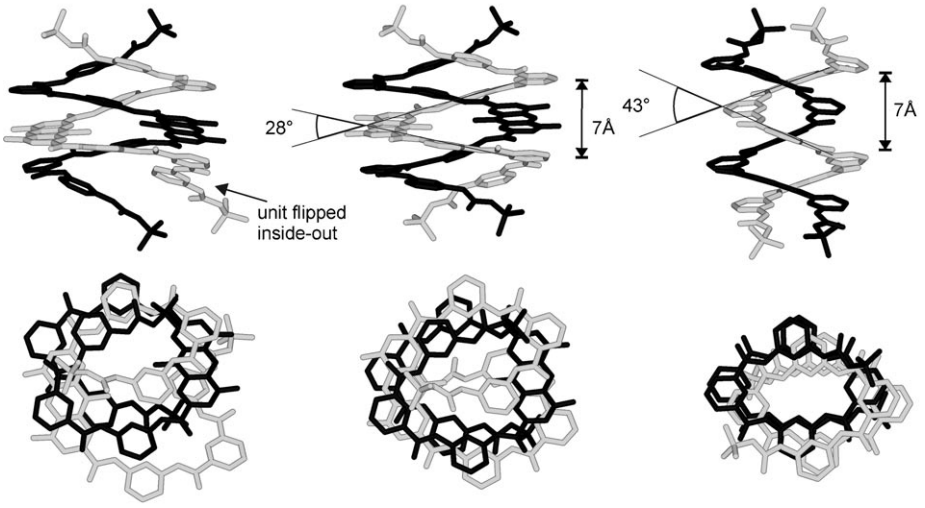

Figure 2. Side views (top row) and top views (bottom row) of the crystal structures of **2** (left and center) and **1**[6] (right) at the same scale. Isobutyl side-chains, hydrogen atoms and included solvent molecules are omitted for clarity. The structures of **2** from crystals grown in DMSO and toluene/hexane are almost superimposable and only one of them is shown in the center. The structure on the left is that from crystals grown from methanol. A comparison between the structures of **2** and the structure of **1** shows that the tilt angle of the strands is lower in $(\mathbf{2})_2$ for the same vertical rise per turn.

The architecture of $(\mathbf{2})_2$ spans two complete helical turns and much resembles the double helical structure of **1** (Figure 2). It possesses a pseudo (noncrystallographic) C_2 symmetry axis that coincides with the helical axis; its double helical pitch is 7 Å, and it has about 4 monomeric units per turn. In toluene/hexane, $(\mathbf{2})_2$ co-crystallizes with two water molecules inside the duplex hollow, although the structure obtained in DMSO does not show any solvent molecule in the helix. Nevertheless, these two structures are almost superimposable and only one of them is shown in Figure 2. Two bifurcated intermolecular hydrogen bonds between pyridine nitrogen atoms and amide NH groups (NH–N distances are in the 2.9–3.1 Å range) are observed at one end of each duplex, as is the case for some oligomers comprised of only pyridine units, such as **1**.[6a] The structures show extensive intermolecular aromatic stacking between the two strands. Each diazaanthracene moiety is sandwiched between the two 2,6-pyridinedicarbonyl units of the other strand. The structure obtained from MeOH shows an unusual misfolding of one terminal amino-pyridine unit, which is flipped inside out of the helix and features an unfavored *s-cis* conformation of the aryl–NHCO linkage. The resulting void space in the helix is filled by a MeOH molecule. Despite this latter difference, the three structures are very similar, suggesting that comparable duplex conformations are reached in polar and nonpolar solvents. As expected, the main difference between $(\mathbf{1})_2$ and $(\mathbf{2})_2$ is the larger diameter of the double helix in $(\mathbf{2})_2$ (Figure 2).

Solution studies: The ^{1}H NMR spectra of **2** in $CDCl_3$, [D6]DMSO, and CD_3OD all show sharp signals corresponding to a single species. Spectra recorded in solvent mixtures have established that the same species occurs in the three solvents (see the Supporting Information). Varying either concentration (from 0.1 to 100 mM) or temperature (from 25 to 90 °C in [D6]DMSO) did not result in significant changes in the spectra of **2**. Together with the solid-state data, this behavior suggests that the species observed in solution is either a double helix with unprecedented robustness, or a single helix that has a very low dimerization constant that nevertheless crystallizes as a duplex. Unequivocal evidence for the first hypothesis is as follows: i) The ESI-MS indicates the presence of a dimeric structure; ii) The ^{1}H NMR signals of the central unit of **2** are shifted upfield ($\Delta\delta$ up to 1 ppm) from expected values, using **9** as a reference, indicative of ring current effects, and thus aromatic stacking, as expected for $(\mathbf{2})_2$, and as is the case for $(\mathbf{1})_2$. Single helical conformers of **1** or **2** are too short for any stacking to involve the central unit; iii) The ROESY correlations are observed between protons that are remote in space in models of the single helical conformation of **2**, but are close in

space in the solid-state structure of $(\mathbf{2})_2$ (Figure 1); iv) If equimolar amounts of **2** and closely related analogue **3** are mixed, signals corresponding to the two species $(\mathbf{2})_2$ and $(\mathbf{3})_3$ are observed in equal proportions along with the signals of a third species, twice as abundant, assigned to a heteroduplex (**2·3**) (Figure 3).

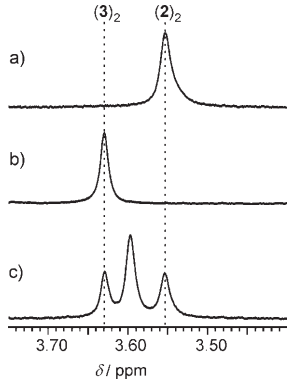

Figure 3. Part of 400 MHz ^{1}H NMR spectra in $CDCl_3$ at 25 °C showing the aryl-CH_3 signals of the 9-methyl-1,8-diazaanthrance units of: a) $(\mathbf{2})_2$; b) $(\mathbf{3})_2$; c) an equimolar mixture of $(\mathbf{2})_2$ and $(\mathbf{3})_2$. Mixing the double helices $(\mathbf{2})_2$ and $(\mathbf{3})_2$ results in the formation of a third species assigned to a heterodimer (**2·3**). The ratio between the three species $(\mathbf{2})_2$, $(\mathbf{3})_2$ and (**2·3**) is 1:1:2, indicates no particular preference for one species or another.

The stability of the double helical dimer of **2** sharply contrasts with all previously described oligomers that consist exclusively of pyridine rings.[6,12] Some of them form duplexes stable to the point that the monomer is not detected by NMR at sub-millimolar concentrations,[12c] but this occurs only at room temperature in solvents that favor hybridization such as $CDCl_3$ or [D8]toluene. Hybridization is weakened upon heating in $CDCl_3$, and is usually moderate in DMSO at room temperature ($K_{dim} < 2000\ L\,mol^{-1}$),[12b] and had simply never been observed in protic solvents.

In order to quantify the K_{dim} values for **2**, we monitored the UV-vis and fluorescence spectral changes upon decreasing the concentration down to 0.5 μM. No change was observed in CH_3OH, DMSO $CHCl_3$ or toluene, suggesting that the K_{dim} values are above 10^7 in these solvents. However, in pyridine, a solvent known to strongly weaken the hybridization of these oligomers, the UV-vis spectra measured at various concentrations revealed the presence of two isosbestic points ($\lambda = 414$ and 434 nm) indicative of a clean transition between two different structures (Figure 4). The moderate hypochromism and small bathochromic shift, observed upon going from a dilute (8.0×10^{-7} M) to a more concentrated solution (1.57×10^{-5} M), are attributed to the transition from a single stranded helical structure to the double helical dimer. Similarly, the fluorescence emission maximum in pyridine is also concentration and temperature dependent ($\Delta\lambda_{max} > 25$ nm). The spectral changes can be fitted to a dimerization isotherm to yield a value of $K_{dim} = 6.5\ 10^5\ L\,mol^{-1}$ at 298 K in this solvent (see the Supporting Information). In contrast, the hybridization of **1** vanishes in polar solvents such as

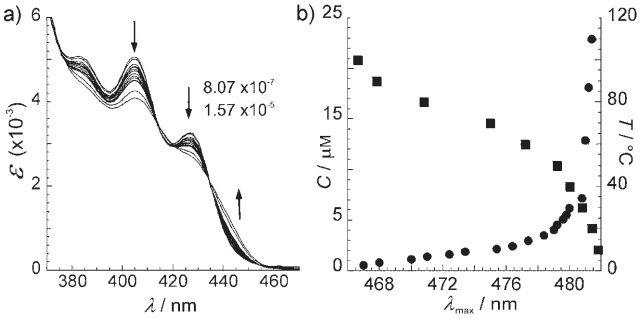

Figure 4. UV-vis spectral features of heptamer **2** in pyridine. a) The absorption spectra at various concentrations (in mol L^{-1}). b) Variation of the wavelength of maximum fluorescence emission upon varying concentration (circles) and temperature (squares).

DMSO and pyridine, even in saturated solutions (25 mM), indicating a K_{dim} value inferior to 1 L mol^{-1}. Thus, in DMSO, the dimerization of **2** is at least 10^7 fold larger than that of **1**, which corresponds to $\Delta\Delta G > 40\ kJ\,mol^{-1}$.

Energy considerations: A Van't Hoff plot of the hybridization of **1** in $CDCl_3$ as observed by NMR gives $\Delta H = -4.4\ kJ\,mol^{-1}$ and $\Delta S = 37\ J\,K^{-1}$. For comparison, a Van't Hoff plot of the hybridization of **2** in pyridine, as observed by fluorescence, gives $\Delta H = -40.2\ kJ\,mol^{-1}$ and $\Delta S = -27.6\ J\,K^{-1}$. Even though these data were collected in different solvents, the small values of ΔS clearly suggest that the very strong hybridization of **2** is of enthalpic origin.

The small values of the entropy of hybridization of $(\mathbf{1})_2$ and $(\mathbf{2})_2$ indicate that the strands undergo hybridization with a minimal loss of motional freedom; the strands are already well-organized as helices in the monomeric state. The positive value for S in the case of $(\mathbf{1})_2$ parallels the behavior of related oligomers,[12b] and suggests that, in this case, solvent effects are at play that make the hybridization entropically favorable. We speculate that the release of water molecules bound in the helix hollows may be at the origin of this phenomenon, if two single helices bind more water molecules than one double helix. Indeed, we have shown that in the case of $(\mathbf{1})_2$, the addition of water disrupts the duplexes,[6b] but we have failed to find any conditions that would efficiently disrupt the duplexes of $(\mathbf{2})_2$.

Aromatic stacking interactions are one of the two main factors expected to contribute to the greater stability of $(\mathbf{2})_2$ compared to $(\mathbf{1})_2$. The augmentation of the π–π stacking surface that occurs upon hybridization is roughly equal to two cross-sections of a helix.[12b,19] It should thus increase as the square of the helix diameter, and lead to a significant stabilization of $(\mathbf{2})_2$. For **2** and **1**, this increase of π–π stacking surface was estimated to be 445 and 329 Å^2, respectively. These two values differ by only 25%. Therefore, aromatic stacking alone accounts for only a small part of the 10 fold increase of the negative enthalpy of hybridization.

A second parameter, maybe less obvious, but definitely more important, that contributes to the strong enthalpy of hybridization of **2**, is the low tilt angle of each strand with

respect to the duplex helical axis (Figure 2). Regardless of helix diameter, the hybridization process requires that each strand undergoes a spring like extension, resulting in a vertical rise of 3.5 Å per turn to reach a double helical pitch of 7 Å (Scheme 1 and Figure 2). This extension is accommodated by an increase of the torsion angles at each amide-aryl linkage, which is enthalpically unfavorable. Such a resistance to torsion is analogous to the material shear modulus G of mechanical springs [Eq. (1)], with the difference that, at the molecular level, torsion causes no stress or fatigue as shearing does in springs subjected to cyclic loading. Heptamers **1** and **2** both possess the same number of torsion angles per helical turn (as springs, they would have identical Gd^4 values). However, the larger diameter of **2** gives rise to a lower tilt angle of the strand, which allows the vertical rise to be accommodated by smaller torsions angles. In the solid state, the average value of the 28 aryl–amide torsions (14 per strand) is 25.4° in $(\mathbf{1})_2$, and 15.7° in $(\mathbf{2})_2$. Molecular mechanics calculations indicate that increasing a pyridine-amide torsion from 15° to 25° has an enthalpic cost superior to 1 kJ mol^{-1} (Figure 5). Since this factor is repeated at each

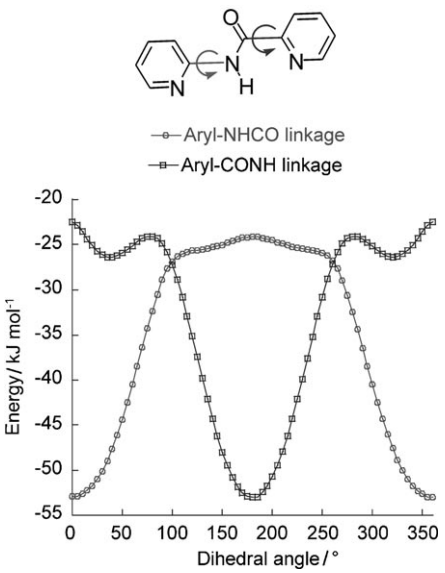

Figure 5. MM-calculated torsion energies for pyridine–NHCO and pyridine–CONH linkages.

aryl–amide linkage (28 times in $(\mathbf{1})_2$ and $(\mathbf{2})_2$) and represents up to 28 kJ mol^{-1}, we believe that it accounts for most of the enthalpic stability of $(\mathbf{2})_2$ with respect to that of $(\mathbf{1})_2$. This result provides evidence that the resistance to elongation depends on helix diameter D in molecular coils as **1** or **2** as it does in springs [Eq. (1)].

The experimental data that we collected concerns the energy differences between monomeric and dimeric helices, and not directly the forces necessary to extend a helically coiled molecule. Discussing the energy differences, as we did here, has allowed us to focus on the role of torsion angles on helix extension, which corresponds to the resistance to shearing in mechanical springs. In fact, intramolecular π–π stacking should, in principle, also be considered as a parameter that contributes to resistance to spring extension, as it is disrupted in the process. This effect could be largely neglected here as it is compensated by intermolecular π–π stacking during double helix formation. However, because of intramolecular π–π stacking, single helices such as **1** and **2** are in fact unlikely to strictly follow Hooke's law; such helices do not have a well-defined spring constant until after the π-stacking is broken. Nevertheless, it can be concluded that the analogy holds between helically folded molecules, such as **1** and **2**, and springs, as far the effect of helix diameter is concerned. It can be speculated that yet wider analogues of **2** comprising several diazaanthracene units would possess an even higher ability to dimerize.

Conclusion

We have shown that enlarging the diameter of a helically folded aromatic amide oligomer by using a 1,8-diazaanthracene monomer instead of a pyridine unit results in a spectacular enhancement of its ability to form a double helical hybrid. The dimerization of the new duplexes exceed 10^7 L mol^{-1} in various organic solvents including methanol, which allows us to speculate that similar behavior may be observed in water, upon functionalizing the oligomer with water solubilizing residues. Such stable complexes represent useful and reliable supramolecular units to construct large discrete or polymeric assemblies. The hybridization process implies a spring-like extension of the helically folded strands to double their pitch. Spring-like extension is mediated (and resisted by) torsions at aryl amide linkages. As in mechanical springs, increasing the helix diameter in molecular helices allows us to produce the same extension at lower torsion angles and thus at a lower enthalpic cost. The lower cost of spring-like extension is apparently at the origin of the remarkable stability of the new helices that are comprised of diazaanthracene units, as compared to the original pyridine oligomers.

Experimental Section

General Procedures and Materials: Unless otherwise noted, the materials were obtained from commercial suppliers and used without further purification. THF was distilled from Na/benzophenone, whereas CH_2Cl_2 and diisopropylethylamine (DIEA) were distilled from CaH_2 prior to use. Chemical shifts are reported in ppm and are calibrated against residual solvent signals of $CDCl_3$ ($\delta = 7.26$, 77.2 ppm), [D$_6$]DMSO ($\delta = 2.50$, 39.4 ppm), or CD_3OD ($\delta = 3.31$, 49.1 ppm). All coupling constants are reported in Hz. Silica gel chromatography was performed by using Merck Kieselgel Si 60. Electrospray ionization (ESI) and high resolution electrospray ionization time of flight (HR-ESI) mass spectra were obtained in the positive ion mode, and matrix assisted laser desorption ionization time of flight (MALDI) mass spectra were obtained in positive ion mode by using α-cyanohydroxycinnamic acid as a matrix.

Dimethyl 1,8-diaza-4,5-diisobutoxy-9-methyl-2,7-anthracene dicarboxylate (5):[15] Under an anhydrous atmosphere and protection from light, compound **4**[14] (1 g, 2.9 mmol) and triphenylphosphine (1.9 g, 7.3 mmol)

were dissolved in anhydrous THF (20 mL) and cooled to 0 °C. Isobutyl alcohol (700 μL) and then diisopropylazadicarboxylate (1.4 mL, 7.3 mmol) were added dropwise at 0 °C. The reaction mixture was stirred for 1 h at 0 °C and then 12 h at 25 °C. It was then evaporated to dryness and the residue was purified by chromatography on silica eluting with toluene/ethyl acetate from 97:3 to 90:10 vol/vol; to obtain **5** (1.6 g, 90 % yield). ^{1}H NMR (300 MHz, $CDCl_3$): $\delta = 9.14$ (s, 1H), 7.50 (s, 2H), 4.13 (d, $J_{(H,H)} = 6.4$ Hz, 4H), 4.10 (s, 6H), 3.50 (s,3H), 2.36 (sept, $J_{(H,H)} = 6.8$ Hz, 2H), 1.20 ppm (d, $J_{(H,H)} = 6.6$ Hz, 12H); ^{13}C NMR (75 MHz, $CDCl_3$): $\delta =$ 166.3, 163.2, 149.6, 145.7, 139.0, 121.4, 113.3, 98.6, 74.9, 53.1, 28.2, 19.1, 13.0 ppm; HRMS(ESI): *m*/*z*: calcd for $C_{25}H_{29}N_2O_6$: 455.2195; found: 455.2182 $[M+H]^+$.

1,8-Diaza-4,5-diisobutoxy-9-methyl-2,7-anthracenedicarbonyl chloride (7):[15] Under an anhydrous atmosphere and protection from light, **5** (1 g, 2.2 mmol) was dissolved in 1,4-dioxane/water (50 mL, 8:2 vol/vol). Sodium hydroxide (220 mg, 5.5 mmol) was added and the reaction was stirred at 25 °C for 12 h. Acetic acid was added until the pH dropped below 7. The dioxane was evaporated and the aqueous solution was extracted with chloroform. The organic phase was dried ($MgSO_4$), filtered, and evaporated by using a toluene azeotrope to yield **6** (930 mg, quantitative), which was used without further purification. ^{1}H NMR (300 MHz, $CDCl_3$): $\delta = 9.71$ (s, 1H), 8.09 (s, 2H), 4.64 (d, $J_{(H,H)} = 6.4$ Hz, 4H), 3.35 (s, 3H), 2.52 (sept, $J_{(H,H)} = 6.8$ Hz, 2H), 1.20 ppm (d, $J_{(H,H)} = 6.6$ Hz, 12H).

Diacid **6** (150 mg) was then suspended in anhydrous $CHCl_3$ (12 mL). 1-Chloro-*N,N*, 2-trimethylpropenylamine (0.12 mL, 0.870, 2.5 equiv) was added and the reaction was stirred at 25 °C for 3 h. The reaction mixture remains a suspension the reaction does reach completion under those conditions. The solvent and the excess reagents were evaporated and the residue was dried in a vacuum line for at least 2 h to yield **7** as a yellow-orange solid. ^{1}H NMR (300 MHz, $CDCl_3$): $\delta = 9.12$ (s, 1H), 7.39 (s, 2H), 3.53 (s, 3H), 2.38 (m, 2H), 1.21 ppm (d, $J_{(H,H)} = 6.6$ Hz, 12H).

Trimeric oligomer 9: Under an anhydrous atmosphere and protection from light, a solution of 2-amino-6-*tert*-butoxycarbonylaminopyridine[16] (430 mg, 2.08 mmol) and *N,N*-diisopropylethylamine (0.16 mL, 2.08 mmol) in anhydrous CH_2Cl_2 (3 mL) was added to freshly prepared **7** (32 mg, 0.7 mmol) suspended in anhydrous CH_2Cl_2 (10 mL) at 0 °C. The reaction was stirred at 0 °C for 30 min and then at 25 °C for 12 h. The mixture was evaporated to dryness and the product was purified by chromatography on SiO_2 eluting with MeOH/CH_2Cl_2 1:99 vol/vol to yield **9** (0.3 g, 53 %) as a yellow powder. ^{1}H NMR (300 MHz, $CDCl_3$): $\delta = 10.66$ (s, 2H), 9.14 (s, 1H), 8.1 (d, $J_{(H,H)} = 7.5$ Hz, 2H), 7.76 (m, 6H), 7.17 (s, 2H), 4.18 (d, $J_{(H,H)} = 6.4$ Hz, 4H), 3.52 (s, 3H), 2.38 (sept, $J_{(H,H)} = 6.8$ Hz, 2H), 1.55 (s, 18H), 1.21 ppm (d, $J_{(H,H)} = 6.6$ Hz, 12H); ^{13}C NMR (75 MHz, $CDCl_3$): $\delta =$ 164.3, 162.9, 152.3, 151.4, 150.7, 149.4, 144.9, 140.8, 121.6, 119.8, 114.2, 114.3, 108.2, 96.45, 81.2, 75.5, 28.4, 19.3 ppm. MS-(ESI): m/*z*: 808.9 $[M+H]^+$, 831.1 $[M+Na]^+$, 1224.0 $[3M+H+Na]^{2+}$, $[3M+2Na]^{2+}$, 1618.1 $[2M+H]^+$, 1639.1 $[2M+H+Na]^+$.

Heptameric oligomer 2: Under an anhydrous atmosphere and protection from light, a solution of boc-monoprotected pyridine trimer **8**[16] (202 mg, 0.45 mmol) and distilled *N,N*-diisopropylethylamine (0.2 mL, 1.1 mmol) in anhydrous THF (6 mL) was added to freshly prepared diacid chloride **7** (98 mg, 0.212 mmol) suspended in anhydrous THF (3 mL) at 0 °C. The reaction was stirred for 30 min at 0 °C and then 12 h at 25 °C. The solvent was removed by evaporation and the residue was purified by means of flash chromatography on silica gel eluting with EtOAc/cycloexane 35:65 to 50:50 vol/vol. Compound **2** (186 mg, 66 %) was obtained as a yellow powder. ^{1}H NMR (300 MHz, $CDCl_3$): $\delta = 10.26$ (s, 2H), 9.13–9.01 (br s, 4H), 8.22 (br d, 2H), 8.13 (s, 1H), 8.04 (d, $J_{(H,H)} = 7.2$ Hz, 2H), 7.90–7.85 (m, 4H), 7.76–7.68 (m, 4H), 7.3 (s, 2H), 7.02–6.9 (m, 4H), 6.75 (br d, 2H), 4.24 (dd, $J_{(H,H)} = 8.4$, 6.3 Hz, 2H), 4.12 (dd, $J_{(H,H)} = 8.4$, 6.3 Hz, 2H), 3.64 (s, 3H), 2.51 (sept, $J_{(H,H)} = 6.8$ Hz, 2H), 1.39 (dd, $J_{(H,H)} = 6.6$, 4.5 Hz, 12H), 0.561 ppm (s, 18H); ^{13}C NMR (75 MHz, $CDCl_3$): $\delta = 163.8$, 161.4, 160.7, 159.7, 152.8, 151.2,150.8, 149.0, 148.9, 148.5, 148.3, 147.5, 143.8, 140.6, 140.0, 138.2, 136.1, 125.7, 125.5, 120.5, 114.2, 110.2, 109.5, 109.4, 108.13, 96.2, 75.3, 28.6, 27.3, 19.5, 19.4, 14.2, 13.0 ppm; HRMS(ESI): *m*/*z*: calcd for $C_{67}H_{69}N_{16}NaO_{12}$: 1289.5281; found: 1289.5205 $[M+Na]^+$.

Heptameric oligomer 3: Under an anhydrous atmosphere and protection from light, a solution of trimeric oligomer **8b** (85 mg, 0.152 mmol) and dry *N,N*-diisopropylethylamine (0.066 mL, 0.37 mmol) in anhydrous THF (2 mL) was added to freshly prepared **7** (32 mg, 0.007 mmol) suspended in THF (1 mL) at 0 °C. The reaction was stirred for 30 min at 0 °C then 12 h at 25 °C. The solvent was removed by evaporation and the residue was purified by flash chromatography on silica gel eluting with EtOAc/CH_2Cl_2 8:92 vol/vol. Compound **3** (75 mg, 71 %) was obtained as a yellow powder. ^{1}H NMR (300 MHz, $CDCl_3$): $\delta = 10.22$ (s, 2H), 9.18–9.00 (br s, 4H), 8.41 (s, 1H), 7.99 (d, $J_{(H,H)} = 7.7$ Hz, 2H), 7.83 (m, 4H), 7.72 (t, $J_{(H,H)} = 6.7$ Hz, 2H), 7.44 (m, 14H), 6.89, (m, 4H), 5.3 (s, 2H), 4.14 (m, 4H), 3.55 (s, 3H), 2.34 (m, 4H), 1.22 (m, 20H), 0.54 ppm (s, 16H); HRMS(ESI): *m*/*z*: calcd for $C_{81}H_{80}N_{16}O_{14}Na$: 1523.5938; found: 1523.5934 $[M+Na]^+$.

X-ray crystallography: Single crystals of heptamer **2** were mounted on a Rigaku R-Axis Rapid diffractometer equipped with a MM007 microfocus rotating anode generator (monochromatized $Cu_{k\alpha}$ radiation, 1.54178 Å). The data collection, unit cell refinement, and data reduction were performed by using the CrystalClear™ software package. The positions of non-H atoms were determined by the program SHELXD, and the position of the H atoms were deduced from coordinates of the non-H atoms and confirmed by Fourier synthesis. H atoms were included for structure factor calculations but not refined.

CCDC-644896 (**2**·toluene/hexane), CCDC-644894 (**2**·DMSO), and CCDC-644895 (**2**·MeOH) contain the supplementary crystallographic data for this paper. These data can be obtained free of charge from The Cambridge Crystallographic Data Centre via www.ccdc.cam.ac.uk/data_request/cif.

NMR studies: The 400 MHz ^{1}H NMR spectra were recorded by using a Bruker–Avance 400 NB US NMR spectrometer by means of a 5 mm direct QNP 1H/X probe with gradient capabilities. The solvent signal was used as an internal reference for these spectra. Samples were not degassed. Rotating frame nuclear Overhauser spectroscopy (ROESY) was used with the following acquisition parameters: 90° pulse-width and transmitter attenuation for the spin-lock pulses were calibrated, P1 = 13 μs, PL1 = 0 dB, spin-lock field strength = 4807 Hz; 1024(t2).512(t1) data points in States-TPPI mode with Z gradients selection and with CW-spin lock for mixing; relaxation delay of 2 s and 40 scans per increment; sweep width of 5200 Hz in both dimensions; mixing time of 250 ms. Processing was done after a sine-bell multiplication in both dimensions, and Fourier transformed in 1 K.1 K real data points. Data processing was performed by using the XWIN-NMR software.

Fluorescence studies: Fluorescence spectra were collected by means of a Shimadzu F4500 spectrofluorometer using a thermostatted cuvette holder ($\lambda_{ex} = 416$ nm) and are uncorrected. The binding isotherms were determined in an aerated pyridine solution at 20 °C by monitoring the fluorescence emission intensity at $\lambda = 484$ and 469 nm as a function of increasing concentration of **2** (from 5.5×10^{-7} M to 2.3×10^{-5} M). To avoid complications from variations in the fluorescence emission envelope owing to changes in the absorption spectrum, ratiometric analysis using least-squares fitting of the data was performed according to Equation (2).

$$[\mathrm{D}] = C_0 \frac{R_F - \lambda_\mathrm{M}}{\lambda_\mathrm{D} - 2\lambda_\mathrm{M}} \qquad (2)$$

The value [D] is the concentration of **2** present in the form of a dimer, C_0 is the total concentration of **2**, R_F is the ratio of fluorescence emission intensity at $\lambda = 484$ and 469 nm, and λ_M and λ_D are the ratio of the products of the molar extinction coefficient and the fluorescence quantum yield (φ) at $\lambda = 484$ and 469 nm for the monomer and dimer of **2**, respectively [Eq. (3)]:

$$\lambda_{\mathrm{D,M}} = \frac{\varepsilon^{484}_{\mathrm{D,M}}\varphi^{484}_{\mathrm{D,M}}}{\varepsilon^{469}_{\mathrm{D,M}}\varphi^{469}_{\mathrm{D,M}}} \qquad (3)$$

The temperature dependence of K_{dim} was obtained in aerated pyridine solution at $[\mathbf{2}] = 1.4\times10^{-4}$ M by evaluating K_{dim} from the relative emission intensity at $\lambda = 484$ and 469 nm using the values of λ_D and λ_M previously obtained from analysis of the binding isotherm. The data was analyzed according to the van't Hoff equation : $\ln K = -\Delta H/RT + \Delta S/R$.

Molecular mechanics calculations: The intramolecular π–π stacking surface of a single helix was estimated by considering the difference between the solvent excluded surface (SES) of an unfolded oligomer and the same oligomer's SES in a helix conformation. The intermolecular π–π stacking surface of a double helix was estimated by considering the difference between the SES of two unfolded oligomers and the SES of the same two oligomers hybridized into a double helix. The conformations of the oligomers were obtained from energy minimization performed with Maestro (v6.5) - Macromodel (v8.6) software.[17] The structures were minimized by using the Truncated Newton Conjugate Gradient (TNCG) method and the MM3* force field in order to obtain local energy minima. The conformations SES were computed with MSMS software[18] by using a probe radius of 1.5 Å (mean radius of a water molecule). The torsion energies of pyridine-NHCO and pyridine-CONH linkages were calculated by using Maestro (v6.5) - Macromodel (v8.6) software through the provided MM3* force field.

Acknowledgements

This work was supported by the CNRS, the Conseil Régional d'Aquitaine, and by an ANR grant (project No. NT05–3_44880). We thank A. Grélard for assistance with our NMR measurements.

[1] For reviews, see: a) T. R. Kelly, *Top. Curr. Chem.* **2005**, *262*, 1–222; b) W. R. Browne, B. L. Feringa, *Nat. Nanotechnol.* **2006**, *1*, 25–35; c) K. Kinbara, T. Aida, *Chem. Rev.* **2005**, *105*, 1377–1400; d) E. R. Kay, D. A. Leigh, F. Zerbetto, *Angew. Chem.* **2006**, *119*, 72–196; *Angew. Chem. Int. Ed.* **2006**, *46*, 72–191; .

[2] *Marks' Standard Handbook for Mechanical Engineers*, 11th ed. (Eds.: E. A. Avallone, T. Baumeister), McGraw-Hill, New York, **1997**.

[3] a) D. J. Hill, M. J. Mio, R. B. Prince, T. S. Hughes, J. S. Moore, *Chem. Rev.* **2001**, *101*, 3893–4011; b) I. Huc, *Eur. J. Org. Chem.* **2004**, 17–29; c) C. Schmuck, *Angew. Chem.* **2003**, *115*, 2552–2556; *Angew. Chem. Int. Ed.* **2003**, *42*, 2448–2452; .

[4] a) C. Bustamante, J. F. Marko, E. D. Siggia, S. Smith, *Science* **1994**, *265*, 1599-1600; b) G. U. Lee, L. A. Chrisey, R. J. Colton, *Science* **1994**, *266*, 771-773; For recent examples, see: c) R. Lohikoski, J. Timonen, A. Laaksonen, *Chem. Phys. Lett.* **2005**, *407*, 23–29; d) T. Lionnet, F. Lankas, *Biophys. J.* **2007**, *92*, L30 L32; e) J. Samuel, S. Sinha, A. Ghosh, *J. Phys. Condens. Matter* **2006**, *18*, S253-S268; f) C. Vaillant, B. Audit, C. Thermes, A. Arneodo, *Phys. Rev. E: Stat., Nonlinear, Soft Matter Phys.* **2003**, *67*, 032901/1–032901/4; studies on the alpha helix have also been reported: g) A. Idiris, M. T. Alam, A. Ikai, *Protein Eng.* **2000**, *13*, 763-770.

[5] H. Goto, H. Katagiri, Y. Furusho, E. Yashima, *J. Am. Chem. Soc.* **2006**, *128*, 7176–7178.

[6] a) V. Berl, I. Huc, R. G. Khoury, M. J. Krische, J.-M. Lehn, *Nature*, **2000**, *407*, 720–723; b) V. Berl, I. Huc, R. G. Khoury, J.-M. Lehn, *Chem. Eur. J.* **2001**, *7*, 2810–2820.

[7] Y. Tanaka, H. Katagiri, Y. Furusho, E. Yashima, *Angew. Chem.* **2005**, *117*, 3935–3938; *Angew. Chem. Int. Ed.* **2005**, *44*, 3867–3870.

[8] a) B. Di Blasio, E. Benedetti, V. Pavone, C. Pedone, *Biopolymers* **1989**, *28*, 203–214; b) D. A. Langs, *Science* **1988**, *241*, 188–189; c) B. M. Burkhart, R. M. Gassman, D. A. Langs, W. A. Pangborn, W. L. Duax, V. Pletnev, *Biopolymers* **1999**, *51*, 129–144.

[9] For recent accounts, see: a) A. Dragulescu-Andrasi, S. Rapireddy, B. M. Frezza, C. Gayathri, R. R. Gil, D. H. Ly, *J. Am. Chem. Soc.* **2006**, *128*, 10258–10267; b) A. Porcheddu, G. Giacomelli, *Curr. Med. Chem.* **2005**, *12*, 2561–2599; c) S. P. Scheidegger, C. J. Leumann, *Chem. Eur. J.* **2006**, *12*, 8014–8023; d) T. Natsume, Y. Ishikawa, K. Dedachi, T. Tsukamoto, N. Kurita, *Chem. Phys. Lett.* **2007**, *434*, 133–138.

[10] a) A. Eschenmoser, *Science* **1999**, *284*, 2118–2124; b) M. Egli, P. S. Pallan, R. Pattanayek, C. J. Wilds, P. Lubini, G. Minasov, M. Dobler, C. J. Leumann, A. Eschenmoser, *J. Am. Chem. Soc.* **2006**, *128*, 10847–10856.

[11] For representative examples, see: a) M. Fujita, K. Umemoto, M. Yoshizawa, N. Fujita, T.; Kusukawa, K. Biradha, *Chem. Commun.* **2001**, 509–518; Kusukawa, K. Biradha, *Chem. Commun.* **2001**, 509–518; b) P. N. W. Baxter, J.-M. Lehn, B. O. Kneisel, G. Baum, D. Fenske, *Chem. Eur. J.* **1999**, *5*, 113–120; c) L. J. Prins, J. J. Verhage, F. de Jong, P. Timmerman, D. N. Reinhoudt, *Chem. Eur. J.* **2002**, *8*, 2302–2313; d) D. Ajami, M. P. Schramm, A. Volonterio, J., Jr. Rebek, *Angew. Chem.* **2007**, *119*, 246–248; Volonterio, J., Jr. Rebek, *Angew. Chem.* **2007**, *119*, 246–248; *Angew. Chem. Int. Ed.* **2007**, *46*, 242–244; .

[12] a) A. Acocella, A. Venturini, F. J. Zerbetto, *J. Am. Chem. Soc.* **2004**, *126*, 2362–2367; b) H. Jiang, V. Maurizot, I. Huc, *Tetrahedron* **2004**, *60*, 10029–10038; c) D. Haldar, H. Jiang, J.-M. Léger, I. Huc, *Angew. Chem.* **2006**, *118*, 5609–5612; *Angew. Chem. Int. Ed.* **2006**, *45*, 5483–5486; ; d) V. Maurizot, J.-M. Léger, P. Guionneau, I. Huc, *Russ. Chem. Bull.* **2004**, *53*, 1572–1576; e) C. Zhan, J.-M. Léger, I. Huc *Angew. Chem.* **2006**, *118, 4741–4744; Angew. Chem. Int. Ed.* **2006**, 45, 4625–4628; *Angew. Chem. Int. Ed.* **2006**, *45*, 4625–4628; ; f) C. Dolain, C. Zhan, J.-M. Léger, I. Huc, *J. Am. Chem. Soc.* **2005**, *127*, 2400–2401; g) D. Haldar, H. Jiang, J.-M. Léger, I. Huc, *Tetrahedron* **2007**, *63*, 6322–6330.

[13] a) J. Garric, J.-M. Léger, I. Huc, *Angew. Chem.* **2005**, *117*, 1990–1994; *Angew. Chem. Int. Ed.* **2005**, *44*, 1954–1958; b) see the preceding paper: J. Garric, J.-M. Léger, I. Huc, *Chem. Eur. J.* **2007**, *13*, 8454–8462.

[14] F. F. Molock, D. W. Boykin, *J. Heterocycl. Chem.* **1983**, *20*, 681–686.

[15] Compounds **4** and derivatives are formally pyrido-quinolines, but their photochemical and photophysical behaviors relate to that of anthracene. These units were thus named diazaanthracenes in this manuscript.

[16] V. Berl, I. Huc, R. G. Khoury, J.-M. Lehn, *Chem. Eur. J.* **2001**, *7*, 2798–2809.

[17] F. Mohamadi, N. G. J. Richards, W.-C. Guida, R. Liskamp, M. Lipton, C. Caufield, G. Chang, T. Hendrickson, W. C. Still, *J. Comput. Chem.* **1990**, *11*, 440–467.

[18] M. F. Sanner, J.-C. Spehner, A. J. Olson, *Biopolymers* **1996**, *38.*, 305–320.

[19] It is equal to the surface involved in intermolecular π–π stacking in a double helix minus the surface of intramolecular π–π stacking in two single helices. See the Experimental Section for details.

Received: June 4, 2007
Published online: July 27, 2007

